

1
2
3
4
5
6
7
8
9
10
11
12
13
14
15
16
17
18
19
20
21
22
23
24
25
26
27
28
29

Engineered biochar as adsorbent for the removal of contaminants from aqueous medium

Stuart Cairns¹, Gabriel Sigmund^{2,3}, Iain Robertson¹, Richard Haine⁴

1 Department of Geography, Swansea University, Singleton Park, Swansea SA2 8PP, UK

2 Environmental Geosciences, Centre for Microbiology and Environmental Systems Science,
University of Vienna, Althanstraße 14, 1090 Vienna, Austria

3 Environmental Analytics, Agroscope, Reckenholzstrasse 191, CH-8046 Zurich,
Switzerland

4 Frog Environmental, Environmental Consultants, The Byre, Blackenhall Park, Bar Ln
DE13 8AJ

Email address of corresponding author: 930112@swansea.ac.uk

ABSTRACT

Biochar is a relatively low cost, sustainable product which can be utilised in the removal of both inorganic and organic contaminants from aqueous media. This chapter outlines the mechanisms of immobilisation for both inorganic and organic contaminants and summarises the key properties that underpin these processes. Immobilisation as a result of cation exchange, complexation, electrostatic interactions, Cation- π bonding, precipitation and reduction is discussed for inorganic contaminants and immobilisation due to H-bonding and charge assisted H-bonding (CAHB), π - π Electron Donor Acceptor (EDA) interaction, electrostatic interaction and steric effect is discussed for organic contaminants. The properties examined include the role of functional groups, cation exchange capacity, specific surface area and pH for inorganic contaminants and specific surface area, aromaticity and polarity for organic contaminants. The effect of raw materials and pyrolysis conditions on these properties is reviewed. Future research needs to bridge the knowledge gained from laboratory work and field work to support the effective use of biochar in real world environments.

30 Key words: biochar, contaminated water, mechanisms, properties, heavy metal, inorganic
31 contaminants, organic contaminants, immobilisation, sorption

32 **Introduction**

33 Biochar is defined as a porous, carbonaceous material that is produced by biomass pyrolysis
34 at temperatures ranging from 350 - 1000°C under limited oxygen conditions (European
35 Biochar Foundation, 2016). During pyrolysis highly aromatic clusters are formed which are
36 responsible for several key features of biochar, specifically it's high chemical stability and
37 high porosity. Biochar is reported to have several functions such as the ability to sequester
38 carbon, enhance soil fertility and remediate environmental contaminants including the
39 removal of contaminants from aqueous media (Inyang *et al.*, 2016; Kätterer *et al.*, 2019). The
40 use of biochar in the remediation of inorganic and organic pollutants has been highlighted for
41 various aqueous media such as road runoff (Cairns *et al.*, 2020), mine waters (Bandara *et al.*,
42 2020), stormwater (Boehm *et al.*, 2020) drinking water (Hu *et al.*, 2019) and biologically
43 treated wastewater (Hagemann *et al.*, 2020). Its attractiveness is further enhanced due to its
44 relatively low cost, simple production process and versatility in utilizing renewable raw
45 material , including biomass waste materials (Ahmad *et al.*, 2014; Zhang *et al.*, 2015;
46 European Biochar Foundation , 2016; Wang *et al.*, 2018b; Xiao *et al.*, 2018).

47 Biochar itself is a reasonably broad term which covers production from a vast number of
48 different biomass raw materials produced at different pyrolytic temperatures yielding biochar
49 with different characteristics. Essentially raw material, pyrolysis and modification such as the
50 addition of minerals, activation or magnetisation alter the efficacy and the mechanisms of the
51 biochar to remediate contaminants in aqueous media. Comparative studies primarily review
52 either raw material, pyrolysis temperature or modified vs unmodified biochar to review

53 sorption capacity or mechanisms (Table 1).

Raw material category	Biochar raw materials	Pyrolysis temperature (°C)	Maximum sorption capacity mg/g	Contaminant(s)	Major removal mechanisms	Author	
Plant Biomass	Oak bark	400 and 450		As, Cd, Pb	ion exchange	Mohan <i>et al.</i> , 2007	
	Pine bark			As, Cd, Pb			
	Oak wood			As, Cd, Pb			
	Pine wood			As, Cd, Pb			
	lucerne shoot	550		Cd, Cu	precipitation, complexation and electrostatic interaction	Bandara <i>et al.</i> , 2020	
	Norway spruce	450-500		Cd, Cu, Pb, Zn	electrostatic attraction	Cairns <i>et al.</i> , 2020	
	Norway spruce	450-500		Cd, Cu, Pb, Zn	electrostatic attraction and precipitation		
	Norway spruce	450-500		Cd, Cu, Pb, Zn	electrostatic attraction and precipitation		
	Tobacco stem	300-700		Cd	cation-pi interaction, precipitation	Zhou <i>et al.</i> , 2018	
				Cu	complexation		
				Pb	Precipitation		
	<i>Canna indica</i>	500	125.8	Cd	precipitates, cation exchange, binding to oxygen-containing groups	Cui <i>et al.</i> , 2016	
	<i>Pennisetum purpureum Schum</i>	500	119.3	Cd	precipitates, cation exchange and binding to oxygen-containing groups		
	KMnO ₄ modified	600	28.1	Cd	surface adsorption	Wang <i>et al.</i> , 2015	
			34.2	Cu	surface adsorption		
			153.1	Pb	surface adsorption		
	Miscanthus	300		11.4	Cd	surface sorption, precipitation	Kim <i>et al.</i> , 2013
		400		11.99	Cd	surface sorption, precipitation	
		500		13.24	Cd	surface sorption, precipitation	
		600		12.96	Cd	surface sorption, precipitation	
honey mesquite	200, 300, 350,			Cd, K	ion exchange, cation-pi bond	Harvey <i>et al.</i> , 2011	
cord- grass	200, 300, 350,			Cd, K			
loblolly pine	200, 300, 350,			Cd, K			
Anaerobically Sugarcane bagasse	600			Cd, Cu, Pb, Ni	precipitation and surface adsorption	Inyang <i>et al.</i> , 2011	
Hardwood mix	600			Cd, Cu, Pb, Ni	surface adsorption		
Straw	450		12.52	Cu	H bonding	Chen <i>et al.</i> , 2011	
			11	Zn	H bonding		
	600		6.79	Cu	H bonding		
			4.54	Zn	H bonding		
Celery	500 and 350	288 - 304		Pb	precipitation, cation exchange and surface complexation	Zhang <i>et al.</i> , 2017	
Wheat straw pellets	550			Ni	cation exchange, electro- static adsorption and surface precipitation	Shen <i>et al.</i> , 2017	
Acacia wood chip	550	4.02		Zn	precipitation, chelation (complexation)	Van Hien <i>et al.</i> , 2020	
Sewage / Manure	Dairy manure	350	7.28-15.68	Cd	complexation, precipitation	Xu, Cao and Zhao, 2013	
			4.16-8.96	Cu			
			13.45-	Pb			
			4.23-9.1	Zn			
	Broiler litter	350 and 700			Cd, Cu, Ni, Pb	coordination by π electrons (CdC) of carbon and precipitation.	Uchimiya <i>et al.</i> , 2010
	Magnetised Sewage sludge	400	249		Pb	electrostatic attraction, ion exchange, complexation, precipitation	Ifthikar <i>et al.</i> , 2017
	Sewage sludge	550	30.88		Pb	coordination with organic hydroxyl and carboxyl functional groups, coprecipitation and complexation	Lu <i>et al.</i> , 2012
	Dairy manure	500	140.76		Pb	precipitation	Cao <i>et al.</i> , 2009
	Food Waste	Nut shells	600		Cd, Pb	ion exchange	Trakal <i>et al.</i> , 2014
		Plum stones			Cd, Pb	ion exchange	
Wheat straws				Cd, Pb	ion exchange		
Grape stalks					Cd, Pb	ion exchange	
Grape husks					Cd, Pb	ion exchange	
Rice husk		350	>54.432		Cd	complexation, precipitation	Xu, Cao and Zhao, 2013
			>31.104		Cu	complexation, precipitation	
			>100.602		Pb	complexation, precipitation	
			>31.59		Zn	complexation, precipitation	
peanut		400			Cr (III)	complexation	Pan <i>et al.</i> , 2013
soybean		400			Cr (III)		
canola		400			Cr (III)		
rice straw		400			Cr (III)		
Sugar Beet Tailing	300	123		Cr (VI)	electrostatic attraction, reduction and complexation	Dong <i>et al.</i> , 2011	
Other	Sediment	400 and 500		Cd, Cu, Pb	cation-pi bond	Dong <i>et al.</i> , 2014	

54

55

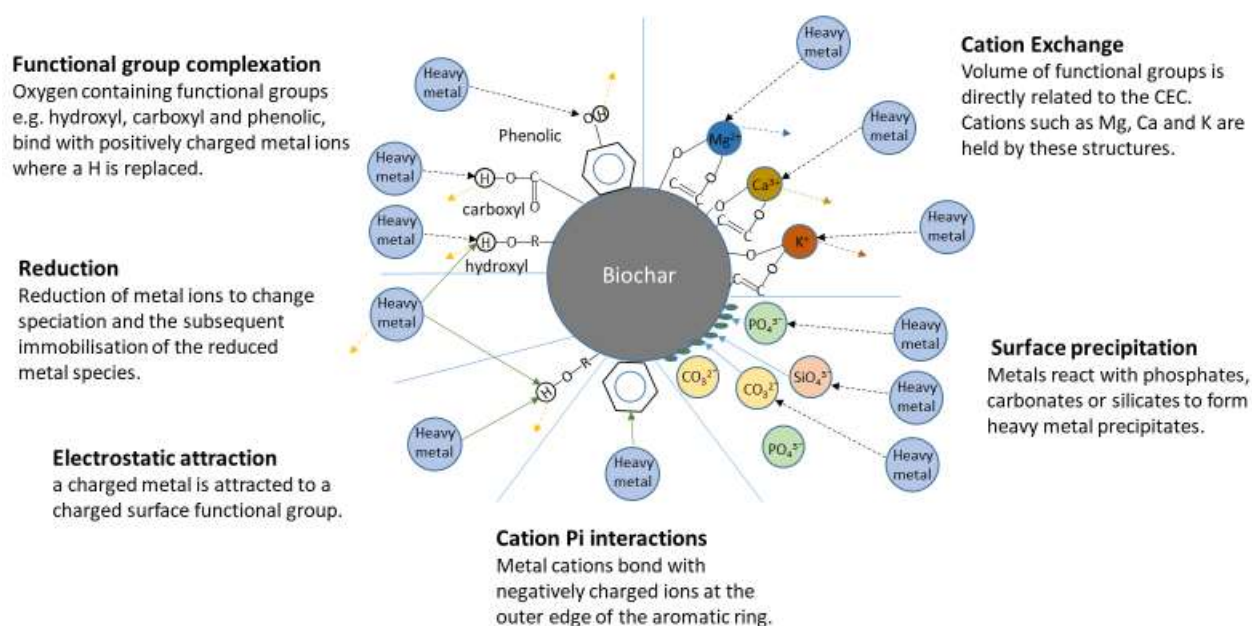
56 Table1. Immobilisation mechanisms of inorganic contaminants by biochar produced from
57 different raw materials

58 Immobilisation of inorganic contaminants

59 The key immobilization mechanisms for inorganic contaminants in aqueous media by biochar
60 are: cation exchange, complexation, electrostatic attraction, cation π bonding, reduction and
61 subsequent sorption, and precipitation (Figure 1). It is worth noting that these mechanisms do
62 not work in isolation and often several mechanisms are relevant at the same time (Ramola et
63 al 2020a).

64

65



66

67 Figure 1. The six major mechanisms of heavy metal immobilization by biochar

68 Cation exchange

69 Cation exchange occurs most notably at early stage adsorption (Mohan *et al.*, 2007;
70 Uchimiya *et al.*, 2010; Iftikhar *et al.*, 2017; Shen *et al.*, 2017) . During cation exchange the
71 biochar releases exchangeable cations such as alkali and alkaline earths, typically Mg, Na, K

72 and Ca (Kumar *et al.*, 2016). These cations are effectively replaced by heavier metal cations
73 found in the aqueous media which bind to the biochar in their stead. Immobilisation
74 mechanisms often do not work in isolation but rather work simultaneously or are intrinsically
75 linked. Studies, such as Mohan *et al.* (2007), cite several other mechanisms working
76 alongside cation exchange in the remediation of inorganic contaminants i.e. precipitation and
77 physical adsorption. In a similar vein cation exchange capacity (CEC) is recognised as being
78 controlled by surface oxygen related functional groups (Trakal, Šigut, *et al.*, 2014; Ding *et al.*,
79 2016), these functional groups also being of great importance in the remediation of
80 inorganic contaminants through complexation.

81 **Complexation**

82 Several authors cite functional group complexation as a major mechanism of immobilization
83 specifically of transition metals such as Cr, Cu and Cd and post transition metals such as Pb
84 (Lu *et al.*, 2012; Pan, Jiang and Xu, 2013; Cui *et al.*, 2016; Peng *et al.*, 2017). Complexation
85 occurs when a H ion is replaced in functional groups such as phenolic, carboxy or hydroxyl
86 (Figure 1) (Xu, Cao and Zhao, 2013; Dong *et al.*, 2014). Complexation is cited in studies
87 with a variety of raw materials including sewage / manure (Weiwen Zhang *et al.*, 2020), food
88 waste such as millet bran (Qiu *et al.*, 2019) and plant biomass (Wang *et al.*, 2018) (Table 1).
89 Again, complexation is often described as working in conjunction with other mechanisms. Lv
90 *et al.* (2018) reported complexation working alongside electrostatic interaction to remove Pb
91 and Cu from aqueous solution.

92 **Electrostatic interactions**

93 Electrostatic interaction occurs between positively charged metals, such as Pb^{2+} , and the
94 negatively charged surface of the biochar, particularly with a proliferation of oxygenated
95 functional groups such as -COOH or -OH (Cui *et al.*, 2015; Lv *et al.*, 2018). Electrostatic
96 attraction is a weaker process than precipitation or complexation and as a result metals
97 immobilised via this mechanism are more susceptible to desorption (Bandara *et al.*, 2020).
98 During their study Bandara *et al.* (2020) described the major mechanisms of Cd and Cu
99 removal as electrostatic interaction with O-containing functional groups, surface
100 complexation and precipitation. Ifthikar *et al.* (2017) also saw electrostatic attraction as being
101 involved in the immobilisation of Pb alongside ion exchange, complexation and precipitation;
102 electrostatic attraction was linked specifically to carboxyl groups. Cui *et al.* (2016) proposed

103 that electrostatic interactions are likely the primary driving force for Cd sorption on wetland
104 plant derived biochar, however even here it is indicated that electrostatic interaction is not the
105 sole mechanism of Cd sorption with complexation playing a role. Ramola et al. (2020 b)
106 found electrostatic interaction to be one of the important mechanisms between Pb ions and
107 mineral groups i.e. bentonite and calcite present in biochar-bentonite composite and biochar-
108 calcite composite respectively prepared at 700°C.

109 **Cation- π bonding**

110 Cation- π bonding is a stabilizing electrostatic interaction of a cation with the polarizable π
111 electron cloud of an aromatic ring. During the pyrolysis of biochar graphene sheets are
112 formed with aromatic structures (Wang *et al.*, 2020). Within these aromatic structures are
113 electron rich domains on the edge of the aromatic structure which have been seen to attract
114 inorganic contaminants such as Cd (Harvey *et al.*, 2011a). Uchimiya *et al.* (2010) recognised
115 the sorptive interactions between d-electrons of metals and aromatic π -electrons of the
116 biochar as one of the primary mechanisms for the retention of Ni and Cd by broiler litter
117 biochar. Xu, Cao, Zhao, *et al.* (2013) also found interactions between d-electrons of metals
118 and aromatic π -electrons when using dairy manure derived biochar, however their study
119 reported that this was important for Zn and Cd remediation but less so for Cu. Kim *et al.*
120 (2013), Yuan *et al.* (2020) and Qiu *et al.* (2019) also recognised the positive impact of
121 aromaticity on adsorption of Cd.

122 **Precipitation**

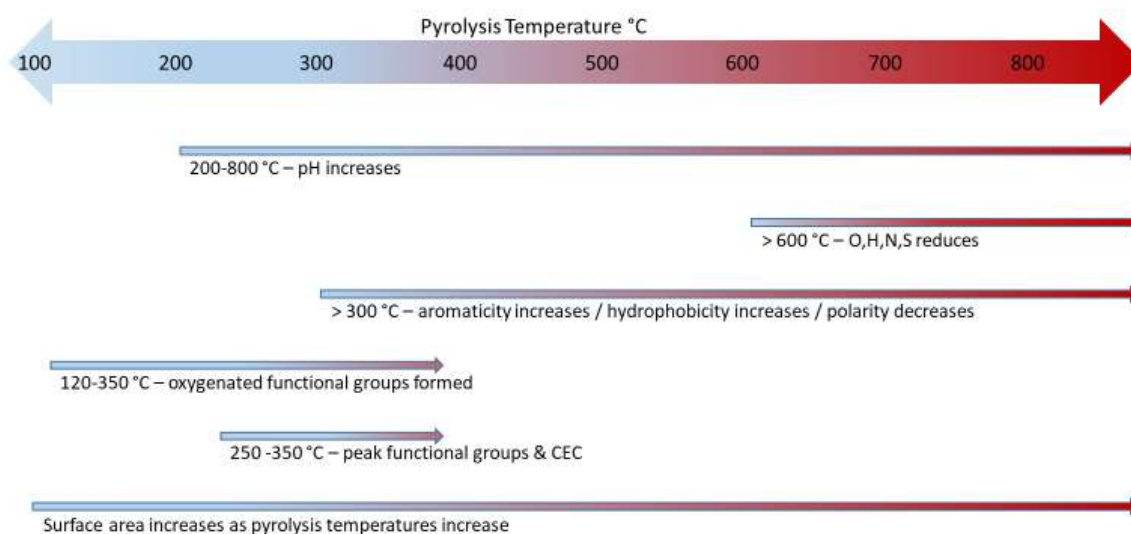
123 In dependence of pH, metals can react with anions including CO_3^{2-} , PO_4^{3-} and SiO_4^{3-} to form
124 solid precipitates (Šrāček and Zeman, 2004). Again raw material is critical to this process
125 being the main driver of the availability of these mineral components (Lu *et al.*, 2012; Xu,
126 Cao and Zhao, 2013). Ifthikar et al. (2017) found silica co-precipitation to be of importance
127 in the remediation of Pb by sewage sludge biochar due to the abundance of silica in the
128 sewage sludge raw material. Precipitation was also significant in Zhang et al.'s (2017) study
129 of celery derived biochar, however due to the characteristics of the raw material carbonate
130 rather than silica co-precipitation was evident. The importance of raw material is further
131 highlighted by Arán *et al.* (2017) who reiterated that the formation of metal carbonates and
132 phosphate precipitates is favoured in biochar from mineral-rich raw material. Several studies
133 assert that precipitation is the primary mechanism for immobilization (Cao and Harris, 2010;

134 Inyang *et al.*, 2012; Lu *et al.*, 2012; Xu, Cao and Zhao, 2013). These studies typically use a
135 raw material of sewage sludge / manure or an amended raw material which provides a high
136 pH and high levels of phosphate and carbonate to be released to precipitate with metals
137 (Inyang *et al.*, 2012). However, precipitation is usually not the sole immobilization
138 mechanism even when such mineral rich raw materials are used. In Xu, Cao and Zhao's
139 (2013) study where P rich dairy manure was used as a raw material, electrostatic attraction
140 and precipitation were both seen to be the governing mechanisms for the removal of Pb, Cu,
141 Zn and Cd. Similarly, Van Hien *et al.*'s study (2020) illustrated the importance of
142 precipitation alongside complexation in the immobilization of Zn.

143 **Reduction**

144 Metals can be reduced by biochar enabling the reduced metal species to be immobilised.
145 Dong *et al.* (2011) reported that due to its high redox potential, Cr(VI) is easily reduced to
146 Cr(III) under acidic conditions in the presence of organic matter. In Dong *et al.*'s study, the
147 immobilisation of Cr occurred by electrostatic attraction of the negatively charged Cr(VI) to
148 positively charged surface sections of a sugar beet biochar and reduction of Cr(VI) to Cr(III)
149 facilitating complexation with functional groups. Cr(VI) reduction to Cr(III) was also
150 reported by Mohan *et al.* (2011) in their study of oak biochar; by products of lignin pyrolysis
151 such as catechol were seen to act as reducing agents as well as being important constituents
152 of units that chelate Cr allowing the biochar to both reduce and bind Cr cations. Klüpfel *et al.*
153 (2014) also highlight the importance of the pyrolysis process by demonstrating that new
154 redox active moieties can be formed in the charring process. Bogusz, Oleszczuk and
155 Dobrowolski, (2015) assert that this reduction can happen in metals with a positive normal
156 potential such as Cu but not with metals such as Cd and Zn that have a negative normal
157 potential.

158 **Key material properties for inorganic contaminant immobilization**



159

160 FIGURE 2. Biochar property changes as a result of pyrolysis temperature

161

162 Functional Groups

163 Surface functional groups of biochar are essential to several immobilisation mechanisms
164 including cation exchange, electrostatic attraction and complexation. Ding *et al.* (2016)
165 discuss the increase in cation exchange of the modified biochar as being resultant from the
166 increase of oxygenated functional groups most notably carboxyl and hydroxyl groups. Other
167 studies, such as Kharel *et al.* (2019) and Huff *et al.* (2018) acknowledge the role of functional
168 groups in cation exchange and have specifically tried to increase carbonyl, carboxyl and
169 hydroxyl groups to increase CEC. Functional groups such as carboxyl and phenolic groups
170 also underpin electrostatic interactions as a charged surface to interact with a given
171 contaminant (Cui *et al.*, 2015). Hydroxyl, carboxyl and phenolic groups also enable
172 complexation to take place when a H ion is replaced by a metal (Trakal, Bingöl, *et al.*, 2014;
173 Wang *et al.*, 2018b). The formation of these functional groups depends on raw material
174 properties and pyrolysis temperature.

175 Trakal *et al.* (2014) suggests that differences in the relevance placed on functional groups can
176 be explained by differences in pyrolysis temperature with studies around 350°C giving
177 greater importance to functional groups and studies around 550-600°C attributing less

178 significance to functional groups as the levels of O reduce. Oxygenated functional groups,
179 such as carboxyl, carbonyl and hydroxyl, start to form at ~120°C in the first stages of
180 pyrolysis where oxygen is more abundant and continue until around 350°C (figure 2) beyond
181 which the O / C ratio is lowered (Lehmann and Joseph, 2009). Studies such as Gray *et al.*
182 (2014) and Wei Zhang *et al.* (2020) have recorded a decrease in these oxygenated functional
183 groups as pyrolysis temperatures rose, with Gray recording a decrease from 370 to 500°C and
184 a further decrease to elimination from 500 °C to 620 °C. Similarly in a comparative study
185 Chen *et al.* (2011) saw that pyrolysis of hardwood at 450 °C resulted in a larger number of
186 functional groups and a higher O/C ratio than straw pyrolyzed at 600 °C. Although
187 temperatures below 450 °C appear to be the best conditions for oxygenated functional
188 groups, at pyrolysis temperatures as high as 600°C the adsorption by hickory wood biochar
189 was still seen to be primarily driven by functional groups (Wang *et al.*, 2015). Whilst raw
190 material and pyrolysis temperature are the primary drivers of the abundance of functional
191 groups they can also increase as a result of oxidation; such oxidation can be a due to natural
192 aging or by chemical oxidation such as with HNO₃-H₂SO₄ or NaOH-H₂O₂ (Fan *et al.*, 2018)

193 **Cation Exchange Capacity**

194 CEC is the key property for sorption through cation exchange. Raw material and pyrolysis
195 temperature are key drivers of CEC (Trakal *et al.*, 2014). Studies show peak CEC to occur at
196 pyrolysis temperatures of 250 – 350°C where functional groups are most abundant, and a
197 diminishing of CEC as pyrolysis temperatures rise past this level (Figure 2), (Harvey *et al.*,
198 2011b). Mohanty *et al.* (2018) concur with the paradigm that low pyrolysis temperature
199 (250–350 °C) lead to high CEC and suggest that this is as a result of the considerable volatile
200 organic matter remaining on biochar rather than it being lost at higher temperatures. If a raw
201 material has high levels of alkali and / or alkaline earths it has the potential for these elements
202 to be available in the biochar for cation exchange. Ifthikar *et al.* (2017) used sewage sludge as
203 a biochar raw material which contained high levels of Ca and Mg, as a result the exchange of
204 these alkaline earth metals was shown to be involved in the early stage adsorption of Pb.
205 Similarly the use of celery biomass as a raw material, which is rich in alkali and alkaline
206 earth metals, resulted in cation exchange playing a significant role in adsorption (T. Zhang *et al.*
207 *et al.*, 2017). Conversely, in studies such as Mantonanaki *et al.* (2016) or Van Hien *et al.* (2020)
208 where the raw material, such as coffee grounds or bamboo, have low levels of Ca, K or Mg,
209 cation exchange is either not highlighted or is described as neither a driver nor a good
210 predictor of adsorption.

211 Specific Surface Area

212 Specific surface area (SSA) is a property of biochar that is very often cited by authors due to
213 its importance in the immobilisation of contaminants in aqueous media; the higher the SSA
214 the more sites are available for sorption to occur. Ifthikar *et al.* (2017) in their study of
215 magnetic sewage sludge biochar, described surface area as critical in the adsorption of Pb.
216 When they compared magnetised and unmagnetised sewage sludge biochar an increase in
217 surface area allowed access to a large number of active sites for remediation to take place
218 increasing removal rates. In their study of oak bark and pine wood biochar, Mohan *et al.*
219 (2007) also suggest that higher adsorption levels were at least partially due to the higher
220 surface area of the oak bark biochar. It is worth noting that a higher surface area does not
221 always result in higher rates of immobilisation particularly if chemisorption rather than
222 physisorption is the driving factor. In studies where precipitation is the major immobilisation
223 mechanism such as Cao and Harris, (2010) and Xu, Cao and Zhao, (2013) surface area is not
224 a major factor. Xu, Cao and Zhao's study (2013) demonstrated that dairy manure biochar had
225 lower surface areas than rice husk biochar ($5.61\text{m}^2\text{g}^{-1}$ vs $27.8\text{m}^2\text{g}^{-1}$) but higher sorption (486
226 mmol kg^{-1} vs $65.5\text{-}140\text{ mmol kg}^{-1}$) as a result of precipitation being the driving mechanism.

227 As with functional groups, surface area is primarily driven by raw material and pyrolysis
228 temperature (figure 2). Wei Zhang *et al.* (2020) describe a surface area increase as a result of
229 temperature increase with rice straw biochar pyrolysed at 400°C having a surface area 0.367
230 m^2g^{-1} which increased to $51.105\text{ m}^2\text{g}^{-1}$ at 700°C . The largest surface area increase occurred
231 between 600 to 700°C with an increase from $8.598\text{ m}^2\text{g}^{-1}$ to $51.105\text{ m}^2\text{g}^{-1}$. Ahmad *et al.*
232 (2012) report a surface area increase from $6\text{m}^2\text{g}^{-1}$ to $448\text{m}^2\text{g}^{-1}$ when temperatures increased
233 from 300 to 700°C . Chen *et al.* (2018) demonstrate an increase from $1.26\text{ m}^2\text{g}^{-1}$ to $351\text{ m}^2\text{g}^{-1}$
234 with an increase in temperature from 300 to 900°C . As explained by Kercher and Nagle,
235 (2003) SSA increases due to the condensation of biomass to graphene like carbon structures
236 forming pyrogenic micro- and mesopores. Hale *et al.* (2016) describe the increase in SSA at
237 high temperatures as a result of amorphous components arranging into turboclastic
238 chrySTALLITES. Chen *et al.* (2011) and Ippolito *et al.* (2020) assert that it is raw material rather
239 than pyrolysis temperatures play the major role in the SSA of biochar.

240

241 pH

242 The pH of biochar is usually alkaline (Lehmann and Joseph, 2015) and as a result it increases
243 and buffers its environments pH. These increases are dependent on raw material and
244 pyrolysis temperatures (figure 2), (Fidel *et al.*, 2017). Studies have shown that the solution
245 pH which effects the metal speciation can be influenced by the pH of the biochar (Cairns *et*
246 *al.*, 2020), the increase in aqueous media pH can induce changes in metal speciation that are
247 favourable for cationic metals such as Pb or Cd and unfavourable for anionic metalloids such
248 as As. The pH of the aqueous solution is cited as one of the main variables affecting the
249 sorption process influencing both the speciation of the metals and the surface charge of the
250 sorbent (Kilic *et al.*, 2013). pH is a key determinant of metal solubility and bioavailability;
251 the more bioavailable a metal is, the more toxic it is to the surrounding ecosystem (Charters,
252 Cochrane and O’Sullivan, 2016). Metals such as Pb and Cd are more mobile at low pH
253 whereas metalloids such as As are more mobile at high pH and as a result the maximum
254 sorption of these metals is seen at different pH (Mohan *et al.*, 2007). Metals that are more
255 mobile at low pH such as Cd, Co, Ni, Pb and Zn are removed best at pH of ~5-6, above pH
256 levels where the metals are mobile (Chen *et al.*, 2011; Lu *et al.*, 2012; Kilic *et al.*, 2013;
257 Trakal, Bingöl, *et al.*, 2014). In contrast, the removal of metalloids that are more mobile at
258 higher pH, such as As, fall when pH is above 8 and the metalloid is more mobile (Navarathna
259 *et al.*, 2019). In terms of cationic heavy metals Lu *et al.* (2012) cited surface charge as being
260 the primary mechanism for Pb sorption and that higher surface charge was driven by
261 increasing pH from 2 to 5. Increasing adsorption was attributed to deprotonation as pH
262 increased. Chen *et al.* (2011) also saw an increase in adsorption until a pH of 5 due to
263 competition between protons and metal cations for sorption sites, with a decrease over pH 5
264 due to the formation of hydroxide complexes. Despite pH 5 being suggested as the pH of
265 maximum sorption by Lu *et al.* (2012) and Chen *et al.* (2011) most studies cite a pH of 6 as
266 being ideal. In their study of activated maple wood biochar Wang *et al.* (2018) saw that with
267 an increasing pH there was an increasing surface charge due to the deprotonation of
268 functional groups up to a pH of 6, above which soluble hydroxyl complexes or surface
269 precipitation formed. Kilic *et al.* (2013) reported similar findings in their study where they
270 saw an increase in electrostatic charge from pH 2 to 6, improving Ni and Co interaction with
271 binding sites. At above pH 6, formation of hydroxylated complexes which compete for active
272 sites were again found. Tran *et al.* (2017) were also in agreement in their study where they
273 investigated the effect of solution pH on the adsorption process of Cu(II) in solutions with pH
274 values from 2.0 to 6.0. They found that up to pH 6 the negative charge of carboxyl groups
275 increased improving adsorption of Cu. Studies also show pH to have an impact on co-

276 precipitation with pH influencing the speciation of metals (Kilic *et al.*, 2013). Inyang *et al.*
277 (2011) suggests that the co-precipitation of Pb and CO_3^{2-} forming hydrocerrusite and cerrusite
278 was as a result of high pH. Similarly Cao and Harris, (2010) note that high pH (~pH 10)
279 allows Pb co-precipitation with both phosphate and carbonate. Biochar pH is effected by
280 pyrolysis temperatures with increases of pH demonstrated from 370 to 600°C (Gray *et al.*,
281 2014), 350 to 750°C (Domingues *et al.*, 2020) and 300 to 700°C (Yuan, Xu and Zhang, 2011;
282 Ahmad *et al.*, 2012). Ramola *et al.* (2020b) found a significant increase in adsorption capacity
283 of biochar-calcite composite prepared at 700 °C, with increase in pH from 3 to 9. This may be
284 because calcite form stronger bond with Pb under alkaline conditions.

285

286

287 **Modification**

288 A number of papers study the effect of modifying biochar to enhance adsorption mechanisms
289 of inorganic contaminants in aqueous media. These modifications generally take the form of
290 activation (creating activated carbon / activated biochar), addition of minerals, or
291 magnetisation.

292 Several studies look to activate the pristine biochar, increasing sorption through an increase
293 in specific surface area (SSA) and modifying surface chemistry, creating activated carbon
294 from biomass sometimes referred to as activated biochar. Methods to chemically activate
295 biochar include the addition of chemicals such as hydrogen peroxide (Wang *et al.*, 2018),
296 sodium hydroxide (Ding *et al.*, 2016) or zinc chloride (Ifthikar *et al.*, 2017). Each of these
297 studies demonstrated an increase in functional groups and surface area leading to an increase
298 in sorption capacity. However, these methods do increase production costs and produce
299 contaminated effluents during production (Hagemann *et al.*, 2020). Physical rather than
300 chemical methods using steam, oxygen or carbon dioxide are also used to increase SSA and
301 remove contaminants (Uchimiya, Isabel M. Lima, *et al.*, 2010; Grycová, Koutník and
302 Prysycz, 2016; Hagemann *et al.*, 2020)

303 The addition of minerals to modify biochar commonly takes place pre pyrolysis such as in
304 Wang *et al's*, (2015) study where potassium permanganate (KMnO_4) was added to increase
305 oxygen functional groups. Under high temperature, KMnO_4 was converted to MnO_x particles

306 onto the surface of the biochar which resulted in an increase in hydroxyl and carboxyl
307 functional groups due to oxidising effect of KMnO_4 . These modifications increased the
308 sorption capacities of biochar by 2.1 times for Pb, 2.8 times for Cu and 5.9 times for Cd. Gan
309 *et al.* (2015) used ZnO modification to adsorb Cr (VI) ions. Again, the raw material was pre-
310 treated with ZnO prior to pyrolysis. The sorption of the modified biochar was 1.2-2 times
311 greater than the sorption of the pristine biochar.

312 Magnetising biochar is a further direction investigated by Yuan *et al.* (2020) Mohan *et al.*
313 (2014) and Chang *et al.* (2006), who introduced Fe^{3+} and / or Fe^{2+} to the pristine biochar to
314 increase the sorption of metals. Magnetisation was carried out with a variety of raw materials
315 including sewage sludge (Ifthikar *et al.*, 2017), oak wood and bark (Mohan *et al.*, 2014) and
316 chitosan (Chang, Chang and Chen, 2006). Each of these studies introduce Fe via solution that
317 is mixed with the biochar and then oven dried to bind the Fe to the surface of the biochar.
318 SSA has been reported to increase with magnetisation in some studies (Chang, Chang and
319 Chen, 2006; Mohan *et al.*, 2014; Ifthikar *et al.*, 2017), however in Mohan *et al.*'s study (2014)
320 this was dependant on raw material with oak bark SSA decreasing with magnetisation but
321 SSA increasing with oak wood magnetisation. Biochar loaded with Fe^{3+} increased the
322 oxygen-containing functional groups and enhanced the ability of complexing Cd (Yuan *et al.*,
323 2020). Ramola *et al.* (2014) observed that iron impregnated tyre biochar (FeTy) was able to
324 remove Pb better than its pristine biochar. The maximum removal of Pb by FeTy was 95%
325 that followed Temkin adsorption isotherm.

326

327 **Immobilization of organic contaminants**

328

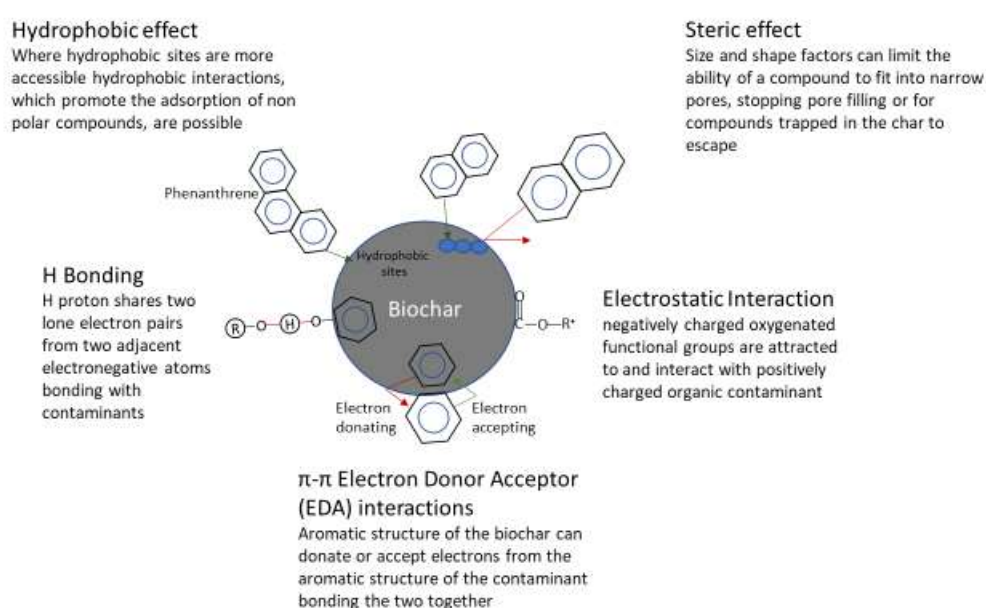
329 As with inorganic contaminants in aqueous media several mechanisms have been
330 documented in the removal of organic contaminants primarily H-bonding and charge assisted
331 H-bonding (CAHB), π - π Electron Donor Acceptor (EDA) interaction, electrostatic interaction
332 and steric effect. These are driven by the structure and properties of the biochar, in particular
333 specific surface area (SSA), aromaticity which can be approximated by the molar H/C ratio
334 and polarity which can be approximated by the molar O/C ratio. Sorption behaviour differs
335 strongly between aromatic and aliphatic compounds, as well as neutral, polar, anionic,
336 cationic and zwitterionic compounds (Hale *et al.*, 2016; Sigmund *et al.*, 2020). The types of

337 organic contaminants found in aqueous media that have attracted the most concern and
338 attention include pesticides, herbicides, polycyclic aromatic hydrocarbons, dyes, and
339 antibiotics which are structurally diverse (Qiu et al., 2009, Beesley et al., 2010, Zheng et al.,
340 2010, Teixidó et al., 2011, Xu et al., 2012).

341

342

343



344

345 Figure 3. The major mechanisms of organic contaminant immobilization by biochar

346 π - π Electron Donor Acceptor Interactions

347 π - π Electron Donor Acceptor (EDA) has been highlighted as one of the most important
348 interactions in the adsorption of aromatic organic compounds to biochar in aqueous media. π -
349 π EDA can occur between π -electron accepting moieties in the centre of the aromatic cluster
350 within the biochar structure and π -electron donating compounds such as phenols or
351 polyaromatic hydrocarbons (PAHs) (Zhu and Pignatello, 2005). The π - π EDA mechanism
352 has been reported as the major mechanism in organic contaminant removal for contaminants
353 including PAHs such as phenanthrene, dibutyl phthalate, sulphides (sulfamethoxazole and

354 sulfapyridine), carbaryl and atrazine (Zhang et al., 2013; Jin et al., 2014; Xie et al., 2014). A
355 study by Ahmed et al (2018) also determined that functionalized biochar can act both as π -
356 electron-donor (sorbing phenanthrene) and π -electron-acceptors (sorbing dinitrobenzene).
357 Therein the π -electron donating sites are located at the outer edges of the graphene like
358 structures within the biochar. For polar contaminants π - π EDA is often reported in
359 conjunction with H-bonding such as in the adsorption of tetracycline, estrone, 17 β -estradiol,
360 estriol, 17 α -ethynylestradiol, bisphenol A and acetate (Saquing, Yu and Chiu, 2016; Zhou *et*
361 *al.*, 2017; Ahmed *et al.*, 2018). The strength of π bonds is in the realm of weak interactions
362 comparable to H-bonds (Pignatello *et al.*, 2017).

363 **H-bonding**

364 H-bonding occurs between a single proton covalently bound to more electronegative atoms
365 and another electronegative atom bearing a lone pair of electrons. Such electronegative atoms
366 can be found on the biochar surface (e.g. O-containing functional groups) (Gilli and Gilli,
367 2010). Studies have highlighted the importance of H-bonding in the removal of several polar
368 organic contaminants such as tetracycline (Jing *et al.*, 2014; Tang *et al.*, 2018), norflurazon
369 and fluridone (Sun *et al.*, 2011) and florfenicol (Zhao and Lang, 2018). Charge assisted H
370 bonding (CAHB) is a special type of H-bonding that occurs when the dissociation constant of
371 the H donor and H acceptor groups are very similar (Δ pKa approaches 0) creating an
372 exceptionally strong H-bond (Li *et al.*, 2013). The formation of negative charge-assisted H
373 bonds have also been reported by Ahmed *et al.* (2017) in the sorption of negative species
374 (sulfonamide antibiotics) from aqueous media. Similarly at a pH of ~8 where deprotonation
375 of the amino group and sulfamido were enhanced, sulfadimine (an antibiotic contaminant)
376 converted to an anion state enabling a strong negative CAHB between sulfadimine and the
377 carboxylate or phenolate functional groups on the biochar (Wan *et al.*, 2020).

378 **Electrostatic interactions**

379 Electrostatic interactions refer to the attraction of oppositely charged groups. For example,
380 negatively charged oxygenated functional groups can bind positively charged organic
381 contaminants, such as methyl violet or methyl blue (Xu *et al.*, 2011; Dawood, Sen and Phan,
382 2017). The charge of the biochar is heavily pH dependant, at pH below the point of zero
383 charge (PZC) the surface charge is positive causing electrostatic repulsion of positively
384 charged contaminants such as sulfadimidine (SMT⁺)(Wan *et al.*, 2020; Ramola et al. 2020a);

385 as the pH of the biochar increases the ionization shifts depending on functional group and
386 compound dissociation constants and the effect of the electrostatic repulsion declines.

387 **Steric effects**

388 Steric effects can influence sorption behaviour of organic compounds. Size and
389 conformational factors may limit the ability of a molecule to fit into narrow pores (pore
390 exclusion), or limit a molecule's approach to sorption sites on the surface (Pignatello, Mitch
391 and Xu, 2017). Removal of organic contaminants from aqueous media by biochar must be
392 considered in conjunction with the pore size of the biochar, the size of the organic
393 contaminant and the shape of the organic contaminant.

394 Size exclusion was reported by

395 K. Yang et al. (2018) in their study of wood chips, rice straw, bamboo chips, cellulose, lignin
396 and chitin biochar. Organic molecules were seen to be restricted and could not access biochar
397 pores smaller than the molecule diameter. Tang et al. (2018) also reported size exclusion in
398 their study of the removal of tetracycline by sewage sludge biochar suggesting that adsorbent
399 shows its best adsorption property when pore diameter is 1.7 – 3 times larger than that of the
400 adsorbate molecule. Schreiter et al. (2018) attributed the higher max sorption capacity for
401 trichloroethylene (TCE) over tetrachloroethylene (PCE) to size exclusion with the smaller
402 TCE molecules able to access a bigger portion of the pore volume of the biochar. Zhang et al.
403 (2013) also conducted a bi-solute study about the removal of carbaryl and atrazine by pig
404 manure biochar. In a similar manner to Schreiter et al. (2018) the higher removal of atrazine
405 was attributed to the smaller molecular size of atrazine compared to carbaryl (0.61 nm versus
406 0.71 nm). Kah *et al.* (2016) also highlighted size exclusion as a phenomenon in their study of
407 a diverse series of sorbents pyrolyzed at different temperatures. Size exclusion was
408 significant for plant derived materials but not so for biochar derived from sewage sludge or
409 pig manure raw materials. These raw materials did not have a microporous structure and as a
410 result did not develop the porosity associated with size exclusion when pyrolyzed. For small
411 molecules, pore filling can occur which is dependent on pore geometry, pore volume and
412 pore size distribution. When these factors are favourable for contaminant condensation in
413 these pores, pore filling can play a dominant role in the immobilisation of organic
414 contaminants (Nguyen *et al.*, 2007; Zhu *et al.*, 2014; Zhao and Lang, 2018). Wang and Xing,
415 (2007) studied the sorption of the hydrophobic compounds phenanthrene and naphthalene
416 and noted that at low solute concentrations, sorption of phenanthrene and naphthalene by
417 biopolymer biochar was dominated by the micropore-filling mechanism; however, with an

418 increase in the solute concentration, immobilisation of these two compounds shifted to a
419 surface-sorption-dominant process.

420

421 **Key material properties for inorganic immobilization**

422 **Specific Surface area**

423 Specific surface area (SSA) is a property of biochar that, as with inorganic immobilisation, is
424 often cited as important for the sorption of organic contaminants as a larger SSA means
425 access to more sorption sites. The larger the SSA, the more opportunity the contaminant has
426 to be removed by the biochar from aqueous media (PrévotEAU et al., 2016). SSA is cited as
427 being a primary property in the removal of organic contaminants in aqueous media by many
428 papers (Zhang et al., 2013; Lattao et al., 2014; Wang et al., 2016; Zhao and Lang, 2018). SSA
429 is driven by pyrolysis temperature and raw material (figure 2). The role of raw material is
430 discussed by Kah et al. (2016) who demonstrate that plant based raw materials can develop
431 micropores, increasing SSA and pore filling potential, but animal waste or sewage based raw
432 materials do not show evidence of such micropore structures. Similarly Wang et al. (2016)
433 highlight that the SSA of plant based biochar was significantly higher than animal based
434 biochar with the result that there were positive correlations between SSA and removal of
435 organic contaminants by wood dust biochar but no such correlations were apparent for swine
436 manure biochar. In their meta data analysis review Ippolito *et al.* (2020) assert that although
437 pyrolysis temperature is important in determining SSA, raw material has the largest influence
438 on SSA with SSA being greatest in wood based biochar. None the less pyrolysis
439 temperatures are still an important tool to control SSA: at higher pyrolysis temperatures
440 amorphous carbons condense to crystalline structures, more pores are formed and volatiles
441 are removed causing a higher SSA (Chen et al., 2012; Zhang et al., 2013; Wang et al., 2016).

442 **Aromaticity**

443 The molar H/C ratio is widely recognised as an index for the degree of aromaticity /
444 carbonisation of biochar which is essential for π - π EDA and hydrophobic interactions. As
445 pyrolysis temperatures increase and aromaticity increases stacks of graphene grow enabling
446 the π - π mechanism to dominate in the removal of contaminants from aqueous media (Jin et
447 al., 2014). Hydrophobic interactions which promote the immobilisation of non-polar /

448 hydrophobic compounds, such as phenanthrene, are also possible where aromatic groups are
449 more accessible (Sun *et al.*, 2013). The hydrophobicity of a contaminant is generally
450 described by the octanol water partition co-efficient (K_{ow}). The aromaticity of biochar is
451 affected by pyrolysis temperature, above $\sim 300^{\circ}\text{C}$ an increase in pyrolysis temperature leads
452 to greater carbonisation and an increase in aromatic compounds (figure 2) (Uchimiya, Isabel
453 M Lima, *et al.*, 2010; Mukherjee, Zimmerman and Harris, 2011; Lehmann and Joseph, 2015;
454 Lou *et al.*, 2016). However, the degree of carbonisation in the biochar is also relevant to
455 partitioning with the partitioning of organic contaminants occurring in the uncarbonized
456 fraction of the biochar (Chen *et al.*, 2018; Schreiter *et al.*, 2018). At lower temperature
457 pyrolysis ($< 400^{\circ}\text{C}$) removal of organic pollutants by biochar is dominated by partitioning due
458 to the amorphous structure of the biochar making them effective media for the partitioning of
459 more polar organic compounds (Chen, Zhou and Zhu, 2008; Sun *et al.*, 2012).

460 **Polarity**

461 The O/C ratio is commonly accepted as an index for polarity and is intrinsically linked to the
462 abundance of oxygenated functional groups. The higher the polarity, and therefore the higher
463 the O/C ratio, the more negatively charged the biochar surface is with the associated benefits
464 for the removal of cations / polar contaminants via H-bonding and electrostatic attraction (Xu
465 *et al.*, 2011; Qiao *et al.*, 2018; Schreiter *et al.*, 2018; Zhao and Lang, 2018). However a high
466 O/C ratio and resultant negative charge can also cause the electrostatic repulsion of anions
467 and can cause water clusters to form around the O-groups repulsing non-polar / hydrophobic
468 contaminants, further demonstrating the importance of the relationship between contaminant
469 structure and properties with the biochar structure and properties (Zhu, Kwon and Pignatello,
470 2005; Rajapaksha *et al.*, 2015; Chen and Ni, 2017; Schreiter *et al.*, 2018). Zhang *et al.* (2017)
471 also discussed the link between partitioning and the polarity of the contaminant with acetone,
472 cyclohexane and toluene partition rates relating directly to polarity; hydrophilic / polar
473 contaminants were adsorbed more easily by biochar that was less polar as the low pyrolysis
474 temperatures lent themselves to the presence of noncarbonized organic matter where
475 partitioning takes place. Polarity, indexed by the O/C ratio, is determined in the main by
476 pyrolysis temperatures; at lower temperatures O is more abundant, and as such the biochar is
477 more polar (figure 2), (Chen and Chen, 2009; X. Zhang *et al.*, 2017).

478 **Limitations**

479 Whilst there is extensive literature on biochar and the removal of organic and inorganic
480 pollutants more research should be conducted to bridge the gap between laboratory results
481 and field work. The majority of research continues to revolve around laboratory findings
482 rather than the use of biochar in the field or in simulated field conditions. Maximum sorption
483 capacity is an important metric however, it represents sorption in perfect conditions such as
484 ideal temperatures, pH, contaminant concentrations and flow. Single contaminant
485 environments are often studied in laboratory batch experiments, yet these conditions are
486 unlikely to be seen in the field where multiple contaminants exist together with dissolved
487 organic matter affecting contaminant mobility, bioavailability and toxicity. The impact of
488 changes in temperature, pH and contaminant concentrations have been studied providing
489 useful insights but very rarely use the parameters as seen in aqueous media where biochar
490 could potentially be deployed such as rivers, runoff or mine waters. Such laboratory findings
491 are not fully transferrable to field conditions which limit their value when attempts are made
492 to use these findings in practice. Whilst the use of simulated field conditions such as storm
493 water, synthetic mine water or even collected mine water has been used to undertake studies
494 in a laboratory setting this approach is far from prevalent.

495

496 **Conclusion and future prospects**

497

498 This chapter highlights the successful use of biochar as an adsorbent for the removal of
499 contaminants from aqueous media. Biochar is a relatively low cost, sustainable product
500 which has been demonstrated to be effective in the removal of both organic and inorganic
501 contaminants. This has led to the study of biochar in relation to aqueous environments such
502 as road runoff (Cairns *et al.*, 2020), mine waters (Bandara *et al.*, 2020), stormwater (Boehm
503 *et al.*, 2020) drinking water (Hu *et al.*, 2019) and biologically treated wastewater (Hagemann
504 *et al.*, 2020). This chapter reviews the key immobilisation mechanisms and underpinning
505 material properties for both inorganic and organic contaminants.

506 The key immobilization mechanisms for inorganic contaminants in aqueous media by biochar
507 are: cation exchange, complexation, electrostatic attraction, cation π bonding, reduction and
508 subsequent sorption, and precipitation. These mechanisms do not work in isolation and it is
509 common for several mechanisms to be relevant simultaneously. Key material properties for

510 inorganic contaminant immobilization include surface functional groups, cation exchange
511 capacity, specific surface area and pH. These material properties are primarily controlled by
512 raw materials and / or pyrolysis temperatures. Surface functional groups of biochar are
513 essential to cation exchange, electrostatic attraction and complexation and are affected by
514 both raw material and pyrolysis temperature. Functional groups start to form at $\sim 120^{\circ}\text{C}$ in the
515 first stages of pyrolysis where oxygen is more abundant and continue until around 350°C .
516 CEC is the key property for sorption through cation exchange. Raw material and pyrolysis
517 temperature are primary drivers of CEC with the lower pyrolysis temperatures allowing more
518 functional groups and as such greater CEC. Specific surface area (SSA) is a further important
519 property of biochar; the higher the SSA the more sites are available for sorption to occur. As
520 opposed to functional groups and CEC, SSA is seen to increase as a result of an increase in
521 pyrolysis temperature. Solution pH, which can be affected by the biochar, is also cited as one
522 of the main variables affecting the sorption process influencing both the speciation of the
523 metals and the surface charge of the sorbent.

524 Several mechanisms have been documented in the removal of organic contaminants from
525 aqueous media, primarily: H-bonding and charge assisted H-bonding (CAHB), π - π Electron
526 Donor Acceptor (EDA) interaction, electrostatic interaction and steric effect. These are
527 driven by the structure and properties of the biochar, in particular specific surface area (SSA),
528 aromaticity which can be approximated by the molar H/C ratio and polarity which can be
529 approximated by the molar O/C ratio. Again, these material properties are primarily
530 controlled by raw materials and / or pyrolysis temperatures. As with inorganic contaminants
531 specific surface area (SSA) is an important property of biochar in relation to the
532 immobilisation of organic contaminants. The molar H/C ratio is an index aromaticity /
533 carbonisation of biochar which is essential for π - π EDA and hydrophobic interactions.
534 Aromaticity increases with pyrolysis temperatures enabling the π - π mechanism to dominate
535 in the removal of contaminants from aqueous media. Hydrophobic interactions which
536 promote the immobilisation of non-polar / hydrophobic compounds are also possible where
537 aromatic groups are more accessible. The O/C ratio, which is commonly accepted as an index
538 for polarity is intrinsically linked to the abundance of oxygenated functional groups. The
539 higher the O/C ratio, the more negatively charged the biochar surface is with the associated
540 benefits for the removal of cations / polar contaminants via H-bonding and electrostatic
541 attraction. However, a high O/C ratio and resultant negative charge can also cause the
542 electrostatic repulsion of anions and can cause water clusters to form around the O-groups

543 repulsing non-polar / hydrophobic contaminants. This highlights the importance of the
544 relationship between contaminant structure and properties with the biochar structure and
545 properties.

546 Studies reviewing the removal of contaminants from aqueous media by biochar in the field
547 are scarce and as a result biochar onsite use in aqueous media necessitates further studies to
548 systematically investigate the interplay of different environmental factors such as pH,
549 dissolved organic matter (DOM) and the mix of contaminants seen in various real world sites.
550 Fouling as a result of these environmental factors could lead to “caking” and the subsequent
551 blocking of biochar surface and pores; such fouling is discussed in the activated carbon
552 community but less so by biochar researchers. A transfer of knowledge between these
553 research communities would help drive meaningful further developments in the field.
554 Furthermore, key material properties of biochar relevant to field conditions are often not
555 reported, including the previously discussed point of zero charge. Understanding the impact
556 of the environmental pH on the charge of the biochar underpins a number of key
557 immobilisation mechanisms and as such arguably should become standard to report bringing
558 laboratory work and field study closer together.

559

560 Acknowledgment

561 Ysgoloriaeth Sgiliau Economi Gwybodaeth (KESS) yn Gymru gyfan sgiliau lefel uwch yn
562 fenter a arweinir gan Brifysgol Bangor ar ran y sector AU yng Nghymru. Fe'i cyllidir yn
563 rhannol gan Gronfeydd Cymdeithasol Ewropeaidd (ESF) cydgyfeirio ar gyfer Gorllewin
564 Cymru a'r Cymoedd.

565

566 Knowledge Economy Skills Scholarships (KESS) is a pan-Wales higher level skills initiative
567 led by Bangor University on behalf of the HE sector in Wales. It is part funded by the Welsh
568 Government's European Social Fund (ESF) convergence programme for West Wales and the
569 Valleys.

570

571 **This work is part funded by the Welsh Government's European Social Fund (ESF)**
572 **convergence programme for West Wales and the Valleys.**

573

574 **Bibliography**

- 575 Ahmad, M. *et al.* (2012) ‘Effects of pyrolysis temperature on soybean stover- and peanut
576 shell-derived biochar properties and TCE adsorption in water’, *Bioresource Technology*, 118,
577 pp. 536–544. doi: 10.1016/j.biortech.2012.05.042.
- 578 Ahmad, M. *et al.* (2014) ‘Biochar as a sorbent for contaminant management in soil and
579 water : A review’, *Chemosphere*, 99, pp. 19–33. doi: 10.1016/j.chemosphere.2013.10.071.
- 580 Ahmed, M. B. *et al.* (2017) ‘Single and competitive sorption properties and mechanism of
581 functionalized biochar for removing sulfonamide antibiotics from water’, *Chemical*
582 *Engineering Journal*, 311, pp. 348–358. doi: 10.1016/j.cej.2016.11.106.
- 583 Ahmed, M. B. *et al.* (2018) ‘Sorption of hydrophobic organic contaminants on functionalized
584 biochar: Protagonist role of π - π electron-donor-acceptor interactions and hydrogen bonds’,
585 *Journal of Hazardous Materials*, 360(August), pp. 270–278. doi:
586 10.1016/j.jhazmat.2018.08.005.
- 587 Arán, D. *et al.* (2017) ‘Use of Waste-Derived Biochar to Remove Copper from Aqueous
588 Solution in a Continuous-Flow System’, *Industrial and Engineering Chemistry Research*,
589 56(44), pp. 12755–12762. doi: 10.1021/acs.iecr.7b03056.
- 590 Bandara, T. *et al.* (2020) ‘Mechanisms for the removal of Cd(II) and Cu(II) from aqueous
591 solution and mine water by biochars derived from agricultural wastes’, *Chemosphere*, 254, p.
592 126745. doi: 10.1016/j.chemosphere.2020.126745.
- 593 Boehm, A. B. *et al.* (2020) ‘Biochar-augmented biofilters to improve pollutant removal from
594 stormwater-can they improve receiving water quality?’, *Environmental Science: Water*
595 *Research and Technology*, 6(6), pp. 1520–1537. doi: 10.1039/d0ew00027b.
- 596 Bogusz, A., Oleszczuk, P. and Dobrowolski, R. (2015) ‘Application of laboratory prepared
597 and commercially available biochars to adsorption of cadmium, copper and zinc ions from
598 water’, *Bioresource Technology*, 196, pp. 540–549. doi: 10.1016/j.biortech.2015.08.006.
- 599 Cairns, S. *et al.* (2020) ‘The removal of lead, copper, zinc and cadmium from aqueous
600 solution by biochar and amended biochars’, *Environmental Science and Pollution Research*,
601 27(17). doi: 10.1007/s11356-020-08706-3.
- 602 Cao, X. and Harris, W. (2010) ‘Properties of dairy-manure-derived biochar pertinent to its

- 603 potential use in remediation', *Bioresource Technology*, 101(14), pp. 5222–5228. doi:
604 10.1016/j.biortech.2010.02.052.
- 605 Chang, Y. C., Chang, S. W. and Chen, D. H. (2006) 'Magnetic chitosan nanoparticles:
606 Studies on chitosan binding and adsorption of Co(II) ions', *Reactive and Functional*
607 *Polymers*, 66(3), pp. 335–341. doi: 10.1016/j.reactfunctpolym.2005.08.006.
- 608 Charters, F. J., Cochrane, T. A. and O'Sullivan, A. D. (2016) 'Untreated runoff quality from
609 roof and road surfaces in a low intensity rainfall climate', *Science of the Total Environment*,
610 550, pp. 265–272. doi: 10.1016/j.scitotenv.2016.01.093.
- 611 Chen, B. and Chen, Z. (2009) 'Sorption of naphthalene and 1-naphthol by biochars of orange
612 peels with different pyrolytic temperatures', *Chemosphere*, 76(1), pp. 127–133. doi:
613 10.1016/j.chemosphere.2009.02.004.
- 614 Chen, B., Zhou, D. and Zhu, L. (2008) 'Transitional Adsorption and Partition of Nonpolar
615 and Polar Aromatic Contaminants by Biochars of Pine Needles with Different Pyrolytic
616 Temperatures', 42(14), pp. 5137–5143. doi: 10.17660/ActaHortic.2009.827.76.
- 617 Chen, W. *et al.* (2018) 'Sorption of chlorinated hydrocarbons to biochars in aqueous
618 environment: Effects of the amorphous carbon structure of biochars and the molecular
619 properties of adsorbates', *Chemosphere*, 210, pp. 753–761. doi:
620 10.1016/j.chemosphere.2018.07.071.
- 621 Chen, W. and Ni, J. (2017) 'Different effects of surface heterogeneous atoms of porous and
622 non-porous carbonaceous materials on adsorption of 1,1,2,2-tetrachloroethane in aqueous
623 environment', *Chemosphere*, 175, pp. 323–331. doi: 10.1016/j.chemosphere.2017.02.067.
- 624 Chen, X. *et al.* (2011) 'Adsorption of copper and zinc by biochars produced from pyrolysis of
625 hardwood and corn straw in aqueous solution', *Bioresource Technology*, 102(19), pp. 8877–
626 8884. doi: 10.1016/j.biortech.2011.06.078.
- 627 Chen, Z. *et al.* (2012) 'Bisolute Sorption and Thermodynamic Behavior of Organic Pollutants
628 to Biomass-derived Biochars at Two Pyrolytic Temperatures'. doi: 10.1021/es303351e.
- 629 Cui, L. *et al.* (2015) 'EDTA functionalized magnetic graphene oxide for removal of Pb(II),
630 Hg(II) and Cu(II) in water treatment: Adsorption mechanism and separation property',
631 *Chemical Engineering Journal*, 281, pp. 1–10. doi: 10.1016/j.cej.2015.06.043.

- 632 Cui, X. *et al.* (2016) ‘Capacity and mechanisms of ammonium and cadmium sorption on
633 different wetland-plant derived biochars’, *Science of the Total Environment*, 539, pp. 566–
634 575. doi: 10.1016/j.scitotenv.2015.09.022.
- 635 Dawood, S., Sen, T. K. and Phan, C. (2017) ‘Synthesis and characterization of slow pyrolysis
636 pine cone bio-char in the removal of organic and inorganic pollutants from aqueous solution
637 by adsorption: Kinetic, equilibrium, mechanism and thermodynamic’, *Bioresource
638 Technology*, 246, pp. 76–81. doi: 10.1016/j.biortech.2017.07.019.
- 639 Ding, Z. *et al.* (2016) ‘Removal of lead, copper, cadmium, zinc, and nickel from aqueous
640 solutions by alkali-modified biochar: Batch and column tests’, *Journal of Industrial and
641 Engineering Chemistry*, 33, pp. 239–245. doi: 10.1016/j.jiec.2015.10.007.
- 642 Domingues, R. R. *et al.* (2020) ‘Enhancing cation exchange capacity of weathered soils using
643 biochar: Feedstock, pyrolysis conditions and addition rate’, *Agronomy*, 10(6), pp. 1–17. doi:
644 10.3390/agronomy10060824.
- 645 Dong, X. *et al.* (2014) ‘The sorption of heavy metals on thermally treated sediments with
646 high organic matter content’, *Bioresource Technology*, 160, pp. 123–128. doi:
647 10.1016/j.biortech.2014.01.006.
- 648 Dong, X., Ma, L. Q. and Li, Y. (2011) ‘Characteristics and mechanisms of hexavalent
649 chromium removal by biochar from sugar beet tailing’, *Journal of Hazardous Materials*,
650 190(1–3), pp. 909–915. doi: 10.1016/j.jhazmat.2011.04.008.
- 651 European Biochar Foundation (EBC) (2016) ‘Guidelines for a Sustainable Production of
652 Biochar’, *European Biochar Foundation (EBC)*, (December), pp. 1–22.
- 653 Fan, Q. *et al.* (2018) ‘Effects of chemical oxidation on surface oxygen-containing functional
654 groups and adsorption behavior of biochar’, *Chemosphere*, 207, pp. 33–40. doi:
655 10.1016/j.chemosphere.2018.05.044.
- 656 Fidel, R. B. *et al.* (2017) ‘Characterization and quantification of biochar alkalinity’,
657 *Chemosphere*, 167, pp. 367–373. doi: 10.1016/j.chemosphere.2016.09.151.
- 658 Gan, C. *et al.* (2015) ‘RSC Advances Cr (VI) adsorption from aqueous solution’, *RSC
659 Advances*, 5, pp. 35107–35115. doi: 10.1039/C5RA04416B.
- 660 Gilli, P. and Gilli, G. (2010) ‘Hydrogen bond models and theories: The dual hydrogen bond

- 661 model and its consequences', *Journal of Molecular Structure*, 972(1–3), pp. 2–10. doi:
662 10.1016/j.molstruc.2010.01.073.
- 663 Gray, M. *et al.* (2014) 'Water uptake in biochars: The roles of porosity and hydrophobicity',
664 *Biomass and Bioenergy*, 61, pp. 196–205. doi: 10.1016/j.biombioe.2013.12.010.
- 665 Grycová, B., Koutník, I. and Prysycz, A. (2016) 'Pyrolysis process for the treatment of food
666 waste', *Bioresource Technology*, 218, pp. 1203–1207. doi: 10.1016/j.biortech.2016.07.064.
- 667 Hagemann, N. *et al.* (2020) 'Wood-based activated biochar to eliminate organic
668 micropollutants from biologically treated wastewater', *The Science of the total environment*,
669 730, p. 138417. doi: 10.1016/j.scitotenv.2020.138417.
- 670 Hale, S. E. *et al.* (2016) 'A synthesis of parameters related to the binding of neutral organic
671 compounds to charcoal', *Chemosphere*, 144, pp. 65–74. doi:
672 10.1016/j.chemosphere.2015.08.047.
- 673 Harvey, Omar R *et al.* (2011) 'Metal Interactions at the Biochar-Water Interface : Energetics
674 and Structure-Sorption Relationships Elucidated by Flow Adsorption Microcalorimetry',
675 *Environmental Science nand Technology*, pp. 5550–5556. doi: 10.1021/es104401h.
- 676 Harvey, Omar R. *et al.* (2011) 'Metal interactions at the biochar-water interface: Energetics
677 and structure-sorption relationships elucidated by flow adsorption microcalorimetry',
678 *Environmental Science and Technology*, 45(13), pp. 5550–5556. doi: 10.1021/es104401h.
- 679 Van Hien, N. *et al.* (2020) 'Effectiveness of different biochar in aqueous zinc removal:
680 Correlation with physicochemical characteristics', *Bioresource Technology Reports*,
681 11(May). doi: 10.1016/j.biteb.2020.100466.
- 682 Hu, Z. *et al.* (2019) 'Preparation of an antibacterial chitosan-coated biochar-nanosilver
683 composite for drinking water purification', *Carbohydrate Polymers*, 219(January), pp. 290–
684 297. doi: 10.1016/j.carbpol.2019.05.017.
- 685 Huff, M. D. *et al.* (2018) 'Surface oxygenation of biochar through ozonization for
686 dramatically enhancing cation exchange capacity', *Bioresources and Bioprocessing*, 5(1).
687 doi: 10.1186/s40643-018-0205-9.
- 688 Ifthikar, J. *et al.* (2017) 'Highly Efficient Lead Distribution by Magnetic Sewage Sludge
689 Biochar: Sorption Mechanisms and Bench Applications', *Bioresource Technology*, 238, pp.

- 690 399–406. doi: 10.1016/j.biortech.2017.03.133.
- 691 Inyang, M. *et al.* (2011) ‘Enhanced Lead Sorption by Biochar Derived from Anaerobically
692 Digested Sugarcane Bagasse’, *Separation Science and Technology*, (September 2013), pp.
693 37–41. doi: 10.1080/01496395.2011.584604.
- 694 Inyang, M. *et al.* (2012) ‘Removal of heavy metals from aqueous solution by biochars
695 derived from anaerobically digested biomass’, *Bioresource Technology*, 110, pp. 50–56. doi:
696 10.1016/j.biortech.2012.01.072.
- 697 Inyang, M. I. *et al.* (2016) ‘A review of biochar as a low-cost adsorbent for aqueous heavy
698 metal removal’, *Critical Reviews in Environmental Science and Technology*, 46(4), pp. 406–
699 433. doi: 10.1080/10643389.2015.1096880.
- 700 Ippolito, J. A. *et al.* (2020) ‘Feedstock choice, pyrolysis temperature and type influence
701 biochar characteristics: a comprehensive meta-data analysis review’, *Biochar*, 2(4), pp. 421–
702 438. doi: 10.1007/s42773-020-00067-x.
- 703 Jin, J. *et al.* (2014) ‘Single-solute and bi-solute sorption of phenanthrene and dibutyl
704 phthalate by plant- and manure-derived biochars’, *Science of the Total Environment*, 473–
705 474, pp. 308–316. doi: 10.1016/j.scitotenv.2013.12.033.
- 706 Jing, X. R. *et al.* (2014) ‘Enhanced adsorption performance of tetracycline in aqueous
707 solutions by methanol-modified biochar’, *Chemical Engineering Journal*, 248, pp. 168–174.
708 doi: 10.1016/j.cej.2014.03.006.
- 709 Kah, M. *et al.* (2016) ‘Pyrolysis of waste materials: Characterization and prediction of
710 sorption potential across a wide range of mineral contents and pyrolysis temperatures’,
711 *Bioresource Technology*, 214, pp. 225–233. doi: 10.1016/j.biortech.2016.04.091.
- 712 Kätterer, T. *et al.* (2019) ‘Biochar addition persistently increased soil fertility and yields in
713 maize-soybean rotations over 10 years in sub-humid regions of Kenya’, *Field Crops
714 Research*, 235(February), pp. 18–26. doi: 10.1016/j.fcr.2019.02.015.
- 715 Kercher, A. K. and Nagle, D. C. (2003) ‘Microstructural evolution during charcoal
716 carbonization by X-ray diffraction analysis’, *Carbon*, 41(1), pp. 15–27. doi: 10.1016/S0008-
717 6223(02)00261-0.
- 718 Kharel, G. *et al.* (2019) ‘Biochar Surface Oxygenation by Ozonization for Super High Cation

- 719 Exchange Capacity’, *ACS Sustainable Chemistry and Engineering*, 7(19), pp. 16410–16418.
720 doi: 10.1021/acssuschemeng.9b03536.
- 721 Kilic, M. *et al.* (2013) ‘Adsorption of heavy metal ions from aqueous solutions by bio-char, a
722 by-product of pyrolysis’, *Applied Surface Science*, 283, pp. 856–862. doi:
723 10.1016/j.apsusc.2013.07.033.
- 724 Kim, W. K. *et al.* (2013) ‘Characterization of cadmium removal from aqueous solution by
725 biochar produced from a giant Miscanthus at different pyrolytic temperatures’, *Bioresource*
726 *Technology*, 138, pp. 266–270. doi: 10.1016/j.biortech.2013.03.186.
- 727 Klüpfel, L. *et al.* (2014) ‘Redox properties of plant biomass-derived black carbon (biochar)’,
728 *Environmental Science and Technology*, 48(10), pp. 5601–5611. doi: 10.1021/es500906d.
- 729 Kumar, A. *et al.* (2016) ‘Production and Utilization of Biochar From Organic Wastes for
730 Pollutant Control on Contaminated Sites’, *Environmental Materials and Waste: Resource*
731 *Recovery and Pollution Prevention*, pp. 91–116. doi: 10.1016/B978-0-12-803837-6.00005-6.
- 732 Lattao, C. *et al.* (2014) ‘Influence of molecular structure and adsorbent properties on sorption
733 of organic compounds to a temperature series of wood chars’, *Environmental Science and*
734 *Technology*, 48(9), pp. 4790–4798. doi: 10.1021/es405096q.
- 735 Lehmann, J. and Joseph, S. (2009) *Biochar for environmental management science and*
736 *technology*. 1st edn. London: Earthscan.
- 737 Lehmann, J. and Joseph, S. (2015) *Biochar for environmental management science,*
738 *technology and implementation*. Second. Abingdon: Routledge.
- 739 Li, X. *et al.* (2013) ‘New insight into adsorption mechanism of ionizable compounds on
740 carbon nanotubes’, *Environmental Science and Technology*, 47(15), pp. 8334–8341. doi:
741 10.1021/es4011042.
- 742 Lou, K. *et al.* (2016) ‘Pyrolysis temperature and steam activation effects on sorption of
743 phosphate on pine sawdust biochars in aqueous solutions’, *Chemical Speciation and*
744 *Bioavailability*, 28(1–4), pp. 42–50. doi: 10.1080/09542299.2016.1165080.
- 745 Lu, H. *et al.* (2012) ‘Relative distribution of Pb²⁺ sorption mechanisms by sludge-derived
746 biochar’, *Water Research*, 46(3), pp. 854–862. doi: 10.1016/j.watres.2011.11.058.

- 747 Lv, D. *et al.* (2018) ‘Application of EDTA-functionalized bamboo activated carbon (BAC)
748 for Pb(II) and Cu(II) removal from aqueous solutions’, *Applied Surface Science*, 428, pp.
749 648–658. doi: 10.1016/j.apsusc.2017.09.151.
- 750 Mantonanaki, A., Pelleri, F.-M. and Gidarakos, E. (2016) ‘Cu (II) AND Pb (II)
751 REMOVAL FROM AQUEOUS SOLUTION USING BIOCHAR’, (September 2016).
- 752 Mohan, D. *et al.* (2007) ‘Sorption of arsenic , cadmium , and lead by chars produced from
753 fast pyrolysis of wood and bark during bio-oil production’, *Journal of Colloid and Interface*
754 *Science*, 310, pp. 57–73. doi: 10.1016/j.jcis.2007.01.020.
- 755 Mohan, D. *et al.* (2011) ‘Modeling and evaluation of chromium remediation from water using
756 low cost bio-char, a green adsorbent’, *Journal of Hazardous Materials*, 188(1–3), pp. 319–
757 333. doi: 10.1016/j.jhazmat.2011.01.127.
- 758 Mohan, D. *et al.* (2014) ‘Cadmium and lead remediation using magnetic oak wood and oak
759 bark fast pyrolysis bio-chars’, *Chemical Engineering Journal*, 236, pp. 513–528. doi:
760 10.1016/j.cej.2013.09.057.
- 761 Mohanty, S. K. *et al.* (2018) ‘Plenty of room for carbon on the ground : Potential applications
762 of biochar for stormwater treatment’, *Science of the Total Environment*, 625, pp. 1644–1658.
763 doi: 10.1016/j.scitotenv.2018.01.037.
- 764 Mukherjee, A., Zimmerman, A. R. and Harris, W. (2011) ‘Surface chemistry variations
765 among a series of laboratory-produced biochars’, *Geoderma*, 163(3–4), pp. 247–255. doi:
766 10.1016/j.geoderma.2011.04.021.
- 767 Navarathna, C. M. *et al.* (2019) ‘Removal of Arsenic(III) from water using magnetite
768 precipitated onto Douglas fir biochar’, *Journal of Environmental Management*, 250(August),
769 p. 109429. doi: 10.1016/j.jenvman.2019.109429.
- 770 Nguyen, T. H. *et al.* (2007) ‘Evidence for a pore-filling mechanism in the adsorption of
771 aromatic hydrocarbons to a natural wood char’, *Environmental Science and Technology*,
772 41(4), pp. 1212–1217. doi: 10.1021/es0617845.
- 773 Pan, J., Jiang, J. and Xu, R. (2013) ‘Adsorption of Cr(III) from acidic solutions by crop straw
774 derived biochars’, *Journal of Environmental Sciences (China)*, 25(10), pp. 1957–1965. doi:
775 10.1016/S1001-0742(12)60305-2.

- 776 Peng, H. *et al.* (2017) 'Enhanced adsorption of Cu(II) and Cd(II) by phosphoric acid-
777 modified biochars', *Environmental Pollution*, 229, pp. 846–853. doi:
778 10.1016/j.envpol.2017.07.004.
- 779 Pignatello, J. J., Mitch, W. A. and Xu, W. (2017) 'Activity and Reactivity of Pyrogenic
780 Carbonaceous Matter toward Organic Compounds', *Environmental Science and Technology*,
781 51(16), pp. 8893–8908. doi: 10.1021/acs.est.7b01088.
- 782 PrévotEAU, A. *et al.* (2016) 'The electron donating capacity of biochar is dramatically
783 underestimated', *Scientific Reports*, 6(June), pp. 1–11. doi: 10.1038/srep32870.
- 784 Qiao, K. *et al.* (2018) 'Preparation of biochar from *Enteromorpha prolifera* and its use for the
785 removal of polycyclic aromatic hydrocarbons (PAHs) from aqueous solution', *Ecotoxicology
786 and Environmental Safety*, 149(July 2017), pp. 80–87. doi: 10.1016/j.ecoenv.2017.11.027.
- 787 Qiu, Y. *et al.* (2019) 'Adsorption of Cd(II) From Aqueous Solutions by Modified Biochars:
788 Comparison of Modification Methods', *Water, Air, and Soil Pollution*, 230(4). doi:
789 10.1007/s11270-019-4135-8.
- 790 Rajapaksha, A. U. *et al.* (2015) 'Enhanced sulfamethazine removal by steam-activated
791 invasive plant-derived biochar', *Journal of Hazardous Materials*, 290, pp. 43–50. doi:
792 10.1016/j.jhazmat.2015.02.046.
- 793 Saquing, J. M., Yu, Y. H. and Chiu, P. C. (2016) 'Wood-Derived Black Carbon (Biochar) as
794 a Microbial Electron Donor and Acceptor', *Environmental Science and Technology Letters*,
795 3(2), pp. 62–66. doi: 10.1021/acs.estlett.5b00354.
- 796 Schreiter, I. J., Schmidt, W. and Schüth, C. (2018) 'Sorption mechanisms of chlorinated
797 hydrocarbons on biochar produced from different feedstocks: Conclusions from single- and
798 bi-solute experiments', *Chemosphere*, 203, pp. 34–43. doi:
799 10.1016/j.chemosphere.2018.03.173.
- 800 Shen, Z. *et al.* (2017) 'Characteristics and mechanisms of nickel adsorption on biochars
801 produced from wheat straw pellets and rice husk', *Environmental Science and Pollution
802 Research*, 24(14), pp. 12809–12819. doi: 10.1007/s11356-017-8847-2.
- 803 Sigmund, G. *et al.* (2020) 'Deep Learning Neural Network Approach for Predicting the
804 Sorption of Ionizable and Polar Organic Pollutants to a Wide Range of Carbonaceous

- 805 Materials', *Environmental Science and Technology*, 54(7), pp. 4583–4591. doi:
806 10.1021/acs.est.9b06287.
- 807 Šráček, O. and Zeman, J. (2004) *Principles of Hydrogeochemistry, Introduction to*
808 *Environmental Hydrogeochemistry*.
- 809 Sun, K. *et al.* (2011) 'Sorption of fluorinated herbicides to plant biomass-derived biochars as
810 a function of molecular structure', *Bioresource Technology*, 102(21), pp. 9897–9903. doi:
811 10.1016/j.biortech.2011.08.036.
- 812 Sun, K. *et al.* (2012) 'Polar and aliphatic domains regulate sorption of phthalic acid esters
813 (PAEs) to biochars', *Bioresource Technology*, 118, pp. 120–127. doi:
814 10.1016/j.biortech.2012.05.008.
- 815 Sun, K. *et al.* (2013) 'Impact of deashing treatment on biochar structural properties and
816 potential sorption mechanisms of phenanthrene', *Environmental Science and Technology*,
817 47(20), pp. 11473–11481. doi: 10.1021/es4026744.
- 818 Tang, L. *et al.* (2018) 'Sustainable efficient adsorbent: Alkali-acid modified magnetic biochar
819 derived from sewage sludge for aqueous organic contaminant removal', *Chemical*
820 *Engineering Journal*, 336(November 2017), pp. 160–169. doi: 10.1016/j.cej.2017.11.048.
- 821 Trakal, L., Šigut, R., *et al.* (2014) 'Copper removal from aqueous solution using biochar:
822 Effect of chemical activation', *Arabian Journal of Chemistry*, 7(1), pp. 43–52. doi:
823 10.1016/j.arabjc.2013.08.001.
- 824 Trakal, L., Bingöl, D., *et al.* (2014) 'Geochemical and spectroscopic investigations of Cd and
825 Pb sorption mechanisms on contrasting biochars : Engineering implications', *Bioresource*
826 *Technology*, 171, pp. 442–451. doi: 10.1016/j.biortech.2014.08.108.
- 827 Tran, H. N. *et al.* (2017) 'Mistakes and inconsistencies regarding adsorption of contaminants
828 from aqueous solutions: A critical review', *Water Research*, 120, pp. 88–116. doi:
829 10.1016/j.watres.2017.04.014.
- 830 Uchimiya, M., Lima, Isabel M., *et al.* (2010) 'Immobilization of Heavy Metal Ions (Cu II, Cd
831 II, Ni II, and Pb II) by Broiler Litter-Derived Biochars in Water and Soil', *Journal of*
832 *Agriculture and Food Chemistry*, pp. 5538–5544. doi: 10.1021/jf9044217.
- 833 Uchimiya, M., Lima, Isabel M., *et al.* (2010) 'Immobilization of heavy metal ions (CuII,

- 834 CdII, NiII, and PbII) by broiler litter-derived biochars in water and soil', *Journal of*
835 *Agricultural and Food Chemistry*, 58(9), pp. 5538–5544. doi: 10.1021/jf9044217.
- 836 Wan, J. *et al.* (2020) 'Characterization and adsorption performance of biochars derived from
837 three key biomass constituents', *Fuel*, 269(October 2019), p. 117142. doi:
838 10.1016/j.fuel.2020.117142.
- 839 Wang, H. *et al.* (2015) 'Removal of Pb (II), Cu (II), and Cd (II) from aqueous solutions
840 by biochar derived from KMnO 4 treated hickory wood', *BIORESOURCE TECHNOLOGY*,
841 197, pp. 356–362. doi: 10.1016/j.biortech.2015.08.132.
- 842 Wang, Q. *et al.* (2018a) 'Sorption and desorption of Pb(II) to biochar as affected by oxidation
843 and pH', *Science of The Total Environment*, 634(May), pp. 188–194. doi:
844 10.1016/j.scitotenv.2018.03.189.
- 845 Wang, Q. *et al.* (2018b) 'Sorption and desorption of Pb (II) to biochar as affected by
846 oxidation and pH', *Science of the Total Environment*, 634, pp. 188–194. doi:
847 10.1016/j.scitotenv.2018.03.189.
- 848 Wang, S. *et al.* (2020) 'Biochar surface complexation and Ni(II), Cu(II), and Cd(II)
849 adsorption in aqueous solutions depend on feedstock type', *Science of the Total Environment*,
850 712, p. 136538. doi: 10.1016/j.scitotenv.2020.136538.
- 851 Wang, X. and Xing, B. (2007) 'Sorption of organic contaminants by biopolymer-derived
852 chars', *Environmental Science and Technology*, 41(24), pp. 8342–8348. doi:
853 10.1021/es071290n.
- 854 Wang, Z. *et al.* (2016) 'Sorption of four hydrophobic organic contaminants by biochars
855 derived from maize straw, wood dust and swine manure at different pyrolytic temperatures',
856 *Chemosphere*, 144, pp. 285–291. doi: 10.1016/j.chemosphere.2015.08.042.
- 857 Xiao, X. *et al.* (2018) 'Insight into Multiple and Multilevel Structures of Biochars and Their
858 Potential Environmental Applications: A Critical Review', *Environmental Science and*
859 *Technology*, 52(9), pp. 5027–5047. doi: 10.1021/acs.est.7b06487.
- 860 Xie, M. *et al.* (2014) 'Adsorption of sulfonamides to demineralized pine wood biochars
861 prepared under different thermochemical conditions', *Environmental Pollution*, 186, pp. 187–
862 194. doi: 10.1016/j.envpol.2013.11.022.

- 863 Xu, R. kou *et al.* (2011) 'Adsorption of methyl violet from aqueous solutions by the biochars
864 derived from crop residues', *Bioresource Technology*, 102(22), pp. 10293–10298. doi:
865 10.1016/j.biortech.2011.08.089.
- 866 Xu, X. *et al.* (2013) 'Removal of Cu, Zn, and Cd from aqueous solutions by the dairy
867 manure-derived biochar', *Environmental Science and Pollution Research*, 20(1), pp. 358–
868 368. doi: 10.1007/s11356-012-0873-5.
- 869 Xu, X., Cao, X. and Zhao, L. (2013) 'Comparison of rice husk- and dairy manure-derived
870 biochars for simultaneously removing heavy metals from aqueous solutions: Role of mineral
871 components in biochars', *Chemosphere*, 92(8), pp. 955–961. doi:
872 10.1016/j.chemosphere.2013.03.009.
- 873 Yang, K. *et al.* (2018) 'Correlations and adsorption mechanisms of aromatic compounds on
874 biochars produced from various biomass at 700 °C', *Environmental Pollution*, 233, pp. 64–
875 70. doi: 10.1016/j.envpol.2017.10.035.
- 876 Yuan, J. H., Xu, R. K. and Zhang, H. (2011) 'The forms of alkalis in the biochar produced
877 from crop residues at different temperatures', *Bioresource Technology*, 102(3), pp. 3488–
878 3497. doi: 10.1016/j.biortech.2010.11.018.
- 879 Yuan, S. *et al.* (2020) 'Contributions and mechanisms of components in modified biochar to
880 adsorb cadmium in aqueous solution', *Science of the Total Environment*, 733, p. 139320. doi:
881 10.1016/j.scitotenv.2020.139320.
- 882 Zhang, F. *et al.* (2015) 'Efficiency and mechanisms of Cd removal from aqueous solution by
883 biochar derived from water hyacinth (*Eichornia crassipes*)', *Journal of Environmental*
884 *Management*, 153, pp. 68–73. doi: 10.1016/j.jenvman.2015.01.043.
- 885 Zhang, H. *et al.* (2017) 'Biomass and Bioenergy Effect of feedstock and pyrolysis
886 temperature on properties of biochar governing end use efficacy', *Biomass and Bioenergy*,
887 105, pp. 136–146. doi: 10.1016/j.biombioe.2017.06.024.
- 888 Zhang, P. *et al.* (2013) 'Adsorption and catalytic hydrolysis of carbaryl and atrazine on pig
889 manure-derived biochars: Impact of structural properties of biochars', *Journal of Hazardous*
890 *Materials*, 244–245, pp. 217–224. doi: 10.1016/j.jhazmat.2012.11.046.
- 891 Zhang, T. *et al.* (2017) 'Efficient removal of lead from solution by celery-derived biochars

- 892 rich in alkaline minerals’, *Bioresource Technology*, 235, pp. 185–192. doi:
893 10.1016/j.biortech.2017.03.109.
- 894 Zhang, Weiwen *et al.* (2020) ‘Comparative study on Pb²⁺ removal from aqueous solutions
895 using biochars derived from cow manure and its vermicompost’, *Science of the Total*
896 *Environment*, 716, p. 137108. doi: 10.1016/j.scitotenv.2020.137108.
- 897 Zhang, Wei *et al.* (2020) ‘Rice waste biochars produced at different pyrolysis temperatures
898 for arsenic and cadmium abatement and detoxification in sediment’, *Chemosphere*, 250, p.
899 126268. doi: 10.1016/j.chemosphere.2020.126268.
- 900 Zhang, X. *et al.* (2017) ‘Biochar for volatile organic compound (VOC) removal: Sorption
901 performance and governing mechanisms’, *Bioresource Technology*, 245(September), pp.
902 606–614. doi: 10.1016/j.biortech.2017.09.025.
- 903 Zhao, H. and Lang, Y. (2018) ‘Adsorption behaviors and mechanisms of florfenicol by
904 magnetic functionalized biochar and reed biochar’, *Journal of the Taiwan Institute of*
905 *Chemical Engineers*, 88, pp. 152–160. doi: 10.1016/j.jtice.2018.03.049.
- 906 Zhou, Y. *et al.* (2017) ‘Modification of biochar derived from sawdust and its application in
907 removal of tetracycline and copper from aqueous solution: Adsorption mechanism and
908 modelling’, *Bioresource Technology*, 245(July), pp. 266–273. doi:
909 10.1016/j.biortech.2017.08.178.
- 910 Zhu, D., Kwon, S. and Pignatello, J. J. (2005) ‘Adsorption of single-ring organic compounds
911 to wood charcoals prepared under different thermochemical conditions’, *Environmental*
912 *Science and Technology*, 39(11), pp. 3990–3998. doi: 10.1021/es050129e.
- 913 Zhu, D. and Pignatello, J. J. (2005) ‘Characterization of aromatic compound sorptive
914 interactions with black carbon (charcoal) assisted by graphite as a model’, *Environmental*
915 *Science and Technology*, 39(7), pp. 2033–2041. doi: 10.1021/es0491376.
- 916 Zhu, X. *et al.* (2014) ‘A novel porous carbon derived from hydrothermal carbon for efficient
917 adsorption of tetracycline’, *Carbon*, 77, pp. 627–636. doi: 10.1016/j.carbon.2014.05.067.
- 918